Gas-Phase Ion−Molecule Reactions between a Series of Protonated Diastereomeric Cavitands and Neutral Amines Studied by ESI-FTICRMS: Gas-Phase Inclusion Complex Formation

J. M. J. Nuutinen,[†] A. Irico,[‡] M. Vincenti,[‡] E. Dalcanale,[§] J. M. H. Pakarinen,[†] and P. Vainiotalo*,[†]

Contribution from the Department of Chemistry, University of Joensuu, P.O. Box 111, FIN-80101 Joensuu, Finland, Dipartimento di Chimica Analitica, Università di Torino, Via Giuria 5, 10125 Torino, Italy, and Dipartimento di Chimica Organica e Industriale, Università di Parma, Parco Area delle Scienze 17/A, 43100 Parma, Italy

Received February 8, 2000

Abstract: Ion−molecule reactions of protonated cavitands with neutral amines have been studied using electrospray ionization (ESI) Fourier transform ion cyclotron resonance (FTICR) mass spectrometry. The cavitands studied are built by bridging a resorcin[4]arene skeleton with four aryl phosphate units. Each of the P=O bonds can be directed toward the inside or the outside of the cavity leading to six stable diastereoisomers. ESI proved to be an effective ionization method for the cavitands, although the range of ionic species observed strongly depended on the orientation of the P=O groups in the isomers and the solvent composition used. Five protonated diastereoisomers were studied in ion−molecule reactions with various types of neutral amines, and the corresponding reaction efficiencies were calculated. The data were compared with that observed for the complexes generated in solution. Collision-induced dissociation (CID) was used to study the structure and relative stability of the complexes formed from different diastereomers both in solution and in the gas phase. The results clearly show that inclusion complexes are formed in the gas phase, but only for some isomers. Although all of the protonated diastereoisomers reacted with amines, the reaction rates were much lower for the diastereoisomers known to form inclusion complexes in solution. When a proton bound dimer was formed, which had the hydrogen bonding established outside the cavity, the reaction took place at the collision rate. Also, CID results confirmed the inclusion complex formation. The cavitand isomers, carrying two or more coordinating P=O groups oriented toward the inside of the cavity, proved to be strong ligands for the charged species, including the proton, organic ammonium ions, and even alkali metal cations, with cesium showing the highest affinity.

Introduction

Host−guest interactions are multiple noncovalent interactions occurring between a large and concave organic molecule (the host) and a small organic or inorganic ion or molecule (the guest), which is embodied within the cavity of the host forming an inclusion complex. Although several noncovalent interactions can occur when the host encloses the guest, usually these interactions are relatively weak. Mass spectrometry is an excellent, and relatively new, technique to the study of host−guest chemistry as a pure bimolecular interaction in the absence of solvents and other interfering species. Mass spectrometry can be used to study host−guest interactions in two different ways: by making the separated host and guest interact in the gas-phase inside the mass spectrometer or by forming the complexes in solution and using the mass spectrometer to reveal them.[1]

Most of the studies so far reported on host−guest interactions in the gas phase have been focused on the complexation between crown ethers and charged guests such as metal ions[2−9] or alkylammonium ions.[10−13] Gas-phase reactivity of ligands other than crown ethers has also been studied, including that of porphyrins,[14] cyclotriynes,[15,16] calixarenes,[17] and valinomycin.[18]

† University of Joensuu.
‡ Università di Torino.
§ Università di Parma.
(1) Vincenti, M. *J. Mass Spectrom.* **1995,** *30,* 925−939.
(2) Zhang, H.; Chu, I.-H.; Leming, S.; Dearden, D. V. *J. Am. Chem. Soc.* **1991,** *112,* 7415−7417.

(3) Zhang, H.; Dearden, D. V. *J. Am. Chem. Soc.* **1992,** *114,* 2754−2755.
(4) Chu, I.-H.; Zhang, H.; Dearden, D. V. *J. Am. Chem. Soc.* **1993,** *115,* 5736−5744.
(5) Dearden, D. V.; Zhang, H. Chu, I.-H.; Wong P.; Chen. Q. *Pure Appl. Chem.* **1993,** *65,* 423−428.
(6) Katrizky, A. R.; Malhotra, N.; Ramanathan, R.; Kemerait, R. C.; Zimmermann, J. A.; Eyler, J. R. *Rapid Commun. Mass Spectrom.* **1992,** *6,* 25−27.
(7) Maleknia, S.; Brodbelt, J. S. *J. Am. Chem. Soc.* **1992,** *114,* 4295−4298.
(8) Maleknia, S.; Brodbelt, J. S. *Rapid Commun. Mass Spectrom.* **1992,** *6,* 376−381.
(9) Liou, C.-C.; Brodbelt, J. S. *J. Am. Soc. Mass Spectrom.* **1992,** *3,* 543−548.
(10) Brodbelt, J. S.; Liou, C.-C. *Pure Appl. Chem.* **1993,** *65,* 409−414.
(11) Liou, C.-C.; Brodbelt, J. S. *J. Am. Chem. Soc.* **1992,** *114,* 6761−6764.
(12) Maleknia, S.; Brodbelt, J. S. *J. Am. Chem. Soc.* **1993,** *115,* 2837−2843.
(13) Liou, C.-C.; Wu, H.-F.; Brodbelt, J. S. *J. Am. Soc. Mass Spectrom.* **1994,** *5,* 260−273.
(14) Ikikura, K. K.; Beauchamp, J. L. *J. Am. Chem. Soc.* **1991,** *113,* 2767−2768.
(15) Dunbar, R. C.; Solooki, D.; Tessier, C. A. Youngs, W. J.; Asamoto, B. *Organometallics* **1991,** *10,* 52−54.

Vincenti and co-workers[19−22] have studied host−guest complexation of some cavitands with neutral organic compounds in the gas phase. Ion−molecule reactions have also been used for chiral host−guest recognition.[23−25] Dalcanale et al.[26−29] have tested cavitands as mass sensitive sensors in the gas phase and in solution. Several kinds of complexes formed in solution have also been investigated using fast atom bombardment (FAB)[30−36] and electrospray ionization (ESI)[37−44] mass spectrometry. Cunniff and Vouros[45] proposed that some cyclodextrin complexes prepared in solution and detected by ESI-MS are possibly not inclusion complexes, but rather electrostatic adducts. The occurrence of these so-called "false positive complexes" have to be taken into consideration when studying noncovalent interaction products formed in solution and ionized by ESI.

In the present work, Fourier transform ion cyclotron resonance mass spectrometry (FTICRMS) was used to study the reactions of neutral amines with protonated diastereomeric cavitands obtained by electrospray ionization (ESI). The main purpose

Scheme 1

Table 1. Abbreviation for the Cavitands Studied

R group[a]	direction of the P=O units					mol wt, g/mol
	iiio[b]	iioo	ioio	iooo	oooo	
H	**1b**					1096.16
CH$_3$	**2b**	**2c**	**2d**	**2e**	**2f**	1152.22
C(CH$_3$)$_3$	**3b**					1320.41

[a] From Scheme 1. [b] i, P=O unit is directed toward the inside of the cavity; o, P=O unit is directed toward the outside of the cavitand.

was to determine whether such protonated cavitands were able to form inclusion complexes with neutral amines in the gas phase. A further objective was to examine whether it was possible to distinguish between real inclusion complexes and electrostatic adducts, namely proton-bound heterodimers in the present case. To compare gas-phase with solution equilibrium data, some complexes were also prepared in solution and analyzed by ESI-MS. The results obtained by ESI were compared with the data observed in earlier FAB experiments.[46] Sodium and potassium ions present in the system as impurities formed complexes with some cavitand isomers. From this finding, the ability of the cavitand isomers to form complexes with the alkali metal ion series was tested, to investigate the actual size of the binding cavity.

The cavitands studied form a series of compounds, built by bridging a resorcin[4]arene skeleton with four aryl phosphate units (Scheme 1). It should be noted that for each phosphate group the P=O bond can be directed either toward the inside of the cavity or toward the outside, leading to six possible diastereoisomers (Scheme 2) which cannot interconvert into one another (Table 1). The isomer **a** having all P=O bonds pointing to the inside cannot be produced easily and was not available for study. Within the series of cavitands examined, the largest cavity is found in isomer **b** and smallest in isomer **f**, since the more P=O bonds are directed outside the narrower the cavity, due to the steric hindrance of the aryl moiety. Dalcanale et al.[47] have determined the X-ray crystal structure for cavitand **2d**, where the distance between two oxygens in opposite P=O groups pointing inside the cavity is 6.29 Å, while the distance is 12.81 Å for outside pointing oxygens. It was also demonstrated that cavitand **2d** has four intramolecular hydrogen bonds

(16) Dunbar, R. C.; Uechi, G. T.; Solooki, D.; Tessier, C. A.; Youngs, W. J.; Asamoto, B. *J. Am. Chem. Soc.* **1993**, *115*, 12477−12482.

(17) Wong, P. S. H.; Yu, X.; Dearden, D. *Inorg. Chim Acta* **1996**, *246*, 259−265.

(18) Wong, P. S. H.; Antonio, B. J.; Dearden, D. V. *J. Am. Soc. Mass Spectrom.* **1994**, *5*, 632−637.

(19) Vincenti, M.; Dalcanale, E.; Soncini, P.; Guglielmetti, G. *J. Am. Chem. Soc.* **1990**, *112*, 445−447.

(20) Vincenti, M.; Pelizzetti, E.; Dalcanale, E.; Soncini, P. *Pure Appl. Chem.* **1993**, *65*, 1507−1512.

(21) Vincenti, M.; Minero, C.; Pelizzetti, E.; Secchi, A.; Dalcanale, E. *Pure Appl. Chem.* **1995**, *67*, 1075−1084.

(22) Vincenti, M.; Dalcanale, E. *J. Chem. Soc., Perkin Trans. 2* **1995**, 1069−1076.

(23) Chu, I.-H.; Dearden, D. V.; Bradshaw, J. S.; Huszthy, P.; Izatt, R. M. *J. Am. Chem. Soc.* **1993**, *115*, 4318−4320.

(24) Dearden, D. V.; Dejsupa, C.; Liang, Y.; Bradshaw, J. S.; Izatt, R. M., *J. Am. Chem. Soc.* **1997**, *119*, 353−359.

(25) Liang, Y.; Bradshaw, J. S.; Izatt, R. M.; Pope, R. M.; Dearden, D. V., *Int. J. Mass Spectrom.* **1999**, *185/186/187*, 977−988.

(26) Nelli, P.; Dalcanale, E.; Faglia, G.; Sberveglieri, G.; Soncini, P. *Sens. Actuators, B* **1993**, *13−14*, 302−304.

(27) Dalcanale, E.; Hartmann, J., *Sens, Actuators, B* **1995**, *24−25*, 39−42.

(28) Hartmann, J.; Hauptmann, P.; Levi, S.; Dalcanale, E. *Sens. Actuators, B* **1996**, *35−36*, 154−157.

(29) Pinalli, R.; Nachtigall, F. F.; Ugozzoli, F.; Dalcanale, E. *Angew. Chem., Int. Ed.* **1999**, *38*, 2377−2380.

(30) Laali, K.; Lattimer, R. P. *J. Org. Chem.* **1989**, *54*, 496−498.

(31) Kurono, S.; Hirano, T.; Tsu-Jimoto, K.; Ohashi, M.; Yoneda, M.; Ohkawa, Y. *Org. Mass Spectrom.* **1992**, *27*, 1157−1160.

(32) Sawada, M.; Shizuma, M.; Takai, Y.; Yamada, H.; Kaneda, T.; Hanafusa, T. *J. Am. Chem. Soc.* **1992**, *114*, 4405−4406.

(33) Langley, G. J.; Kilburn, J. D.; Flack, S. S. *Org. Mass Spectrom.* **1993**, *28*, 478−480.

(34) Sawada, M.; Okumura, Y.; Shizuma, M.; Takai, Y.; Hidaka, Y.; Yamada, H.; Tanaka, T.; Kaneda, T.; Hirose, K.; Misumi, S.; Takahashi, S. *J. Am. Chem. Soc.* **1993**, *115*, 7381−7388.

(35) Mele, A.; Panzeri, W.; Selva, A. *Eur. Mass Spectrom.* **1997**, *3*, 347−354.

(36) Reiche, K. B.; Starke, I.; Kleinpeter, E.; Holdt, H.-J. *Rapid Mass Spectrom.* **1998**, *12*, 1021−1027.

(37) Lippmann, T.; Wilde, H.; Pink, M.; Schäfer, A.; Hesse, M.; Mann, G. *Angew. Chem., Int. Ed. Engl.* **1993**, *32*, 1195−1197.

(38) Haskins, N. J.; Saunders, M. R.; Camilleri, P. *Rapid Commun. Mass Spectrom.* **1994**, *8*, 423−426.

(39) Colton, R.; Mitchell, S.; Traeger, J. C. *Inorg. Chim. Acta* **1995**, *231*, 87−93.

(40) Bakhtiar, R.; Kaifer, A. E. *Rapid Commun. Mass Spectrom.* **1998**, *12*, 111−114.

(41) Young, D.-S.; Hung, H.-Y.; Kao Liu, L. *Rapid Commun. Mass Spectrom.* **1997**, *11*, 769−773.

(42) Schalley, C. A.; Rivera, J. M.; Martín, T.; Santamaría, J.; Siuzdak, G.; Rebek, J., Jr. *Eur. J. Org. Chem.* **1999**, 1325−1331.

(43) Schalley, C. A.; Martín, T.; Obst, U.; Rebek, J., Jr. *J. Am. Chem. Soc.* **1999**, *121*, 2133−2138.

(44) Schalley, C. A.; Castello, R. K.; Brody, M. S.; Rudkevich, D. M.; Siuzdak, G.; Rebek, J., Jr. *J. Am. Chem. Soc.* **1999**, *121*, 4568−4579.

(45) Cunniff, J. B.; Vouros, P. *J. Am. Soc. Mass Spectrom.* **1995**, *6*, 437−447.

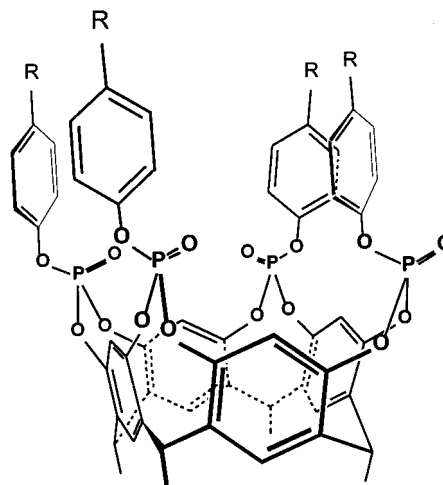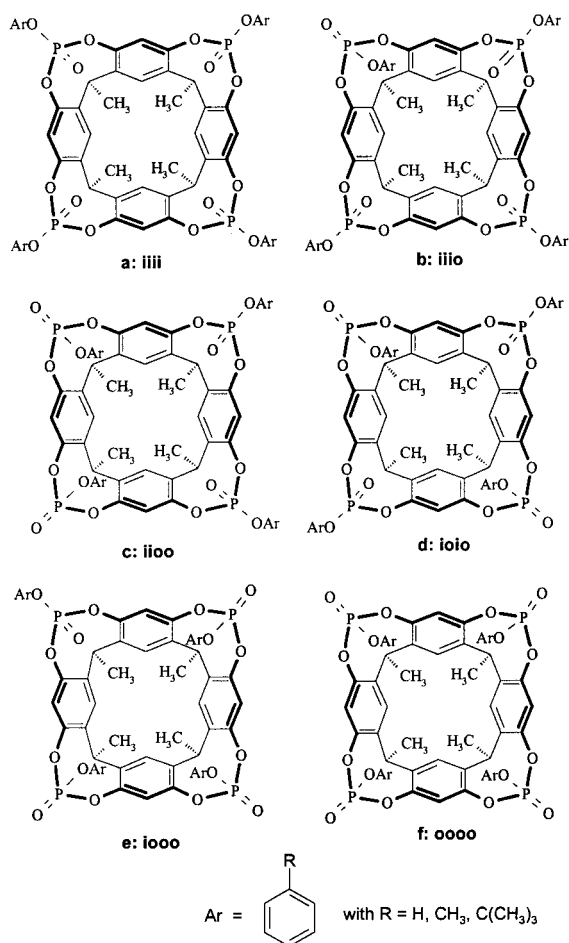(46) Vincenti, M.; Irico, A.; Dalcanale, E. *Advances in Mass Spectrometry*; Karjalainen, E. J., Hesso, A. E., Jalonen, J. E., Karjalainen, U. P., Eds.; Elsevier Science Publishers B.V.: Amsterdam, 1998; Vol. 14; pp 129−150.

(47) Dalcanale, E.; Jacopozzi, P.; Ugozzoli, F.; Mann, G. *Supramol. Chem.* **1998**, *9*, 305−316.

Scheme 2

a: iiii

b: iiio

c: iioo

d: ioio

e: iooo

f: oooo

Ar =

with R = H, CH$_3$, C(CH$_3$)$_3$

involving the tolyl *ortho* hydrogens and the phosphate oxygens that extend the walls of the cavity without closing it. Although the information conveyed by X-ray data cannot be directly transferred into the gas phase, it still holds for describing the general features.

In the previous studies conducted in solution and under FAB conditions,[46,48] the binding capability of the neutral isomers (**2b**, **2c**, **2d**, **2e**, **2f**) was tested. The reactions were carried out with alkyl- and arylammonium ions and showed decreasing binding properties along the isomer series, from the cavitand carrying three converging P=O bonds (**2b**) to the one with no converging P=O bonds (**2f**).

Experimental Section

Mass Spectrometry. All electrospray experiments were performed using a Fourier transform ion cyclotron resonance mass spectrometer (Bruker BioApex 47e, Bruker Daltonics, Billerica, USA), equipped with a 4.7 T, 160 mm bore superconducting magnet (Magnex Scientific Ltd., Abingdon, UK), Infinity cell, and interfaced to an electrospray ionization source (Analytica of Branford Inc. Branford, USA) having an on- and off-axis spray needle. The vacuum is maintained by rotary vacuum pumps followed by turbomolecular pumps each supplied by Edwards (Edwards High Vacuum International, Crawley, UK) in four different regions: electrospray source, ion source, ion optical area, and cell region. With the electrospray source in operation, a base pressure of 5 × 10^{-10} Torr in the cell region was achieved. The ions were focused through different pressure regions by the RF-only hexapole ion guide and transferred to the ion cyclotron resonance cell for trapping and

detection. The instrument was calibrated externally using a water: acetonitrile solution of sodium trifluoroacetate, as introduced by Moini et al.[49] Scan accumulation and data processing were performed with XMASS 4.0.1 software on a Silicon Graphics (Silicon Graphics, Inc., Mountain View, CA) INDY 180 MHz MIPS R5000 computer.

The sample solution was continuously introduced into the interface sprayer by a syringe infusion pump at a flow rate of 50 μL/h under atmospheric pressure. Experiments were performed using the on-axis needle and applying a potential of −3.5 kV to the entrance of the glass capillary, the end plate, and the cylinder. The potential on the glass capillary exit was set at 50−375 V. The charged droplets were dried with nitrogen at a temperature of 500 K in the interface region between the grounded needle and the nickel (in some measurements platinum) coated glass capillary. All source voltages were adjusted to optimize the signal. The host cavitand molecules were electrosprayed, and the resulting ions were guided into the trapping cell and captured.

When ion−molecule reactions were studied, neutral amines were introduced in to the cell using a precision variable leak valve (Varian, Palo Alto, USA) until 5.0 × 10^{-8} Torr pressure was observed. The pressure readings were corrected for the sensitivity of the ion gauge toward each neutral reagent and for the pressure gradient between the cell and the ion gauge.[50] The latter correction factor was obtained by measuring the rates of reactions with known rate constants for neutral propylamine. Argon was introduced in to the cell through a pulsed valve for cooling the cavitand ions formed under electrospray. After a 1 s delay time, the cooled protonated host ions were isolated using the correlated harmonic excitation field (CHEF) procedure.[51] The isolated ions were allowed to react with the neutral amine for variable reaction times up to 60 s, before the product ions were detected. All the data was background corrected. The decay of the relative abundance of the reactant ion as a function of time was used to deduce the reaction rate constant (k). Relative reaction efficiencies (K_{eff}) were calculated using ADO theory proposed by Bowers et al.[52] (efficiency = reaction rate/ collision rate). The [product ion]/[reactant ion] ratio, [M + H + amine]$^+$/[M + H]$^+$, was determined after the reaction had approached the equilibrium. The attainment of equilibrium was verified by continuing the reaction until the ratio between the [M + H + amine]$^+$ and [M + H]$^+$ ion intensities became constant.

In collision-induced dissociation (CID) experiments, cooled precursor ions were isolated using the CHEF procedure. The ions were translationally excited by an on-resonance radio frequency (RF) pulse and allowed to undergo multiple collisions with pulsed background argon gas. The excited ions were allowed to collide and dissociate during 1 or 5 s delay times, after which the CID spectrum was recorded.

Theoretical Methods. The molecular mechanics studies and the investigation of ab initio optimized structure were carried out on a Silicon Graphics Indigo workstation using Sybyl[53] molecular mechanics software. The systematic conformational analysis was carried out using the Search module within Sybyl. The lowest energy Sybyl optimized structure was used as a starting point for ab initio molecular orbital calculation. Ab initio calculation was performed with the Gaussian98[54] series of programs on Silicon Graphics Indigo hardware (SGI Origin

(48) Vincenti, M.; Dalcanale, E. *Proceedings of The 44th ASMS Conference on Mass Spectrometry and Allied Topics*, Portland, OR, May 12−16, 1996, p 143.

(49) Moini, M.; Jones, B. L.; Rogers, R. M.; Jiang, L. *J. Am. Soc. Mass Spectrom.* **1998**, *9*, 977−980.

(50) Bartmess, J. E.; Georgiadis, R. M. *Vacuum* **1983**, *33*, 149−153.

(51) de Koning, L. J.; Nibbering, N. M. M.; van Orden, S. L.; Laukien, F. H. *Int. J. Mass Spectrom. Ion Processes* **1997**, *165/166*, 209−219.

(52) Su, T.; Bowers, M. T. In *Gas-Phase Ion Chemistry*; Bowers, M. T., Ed.; Academic Press: New York, 1979; p 83.

(53) Tripos Associates, Inc., St. Louis, MO.

(54) Gaussian98: Frisch, M. J.; Trucks, G. W.; Schlegel, H. B.; Scuseria, G. E.; Robb, M. A.; Cheeseman, J. R.; Zakrzewski, V. G.; Montgomery, Jr. J. A.; Stratmann, R. E.; Burant, J. C.; Dapprich, S.; Millam, J. M.; Daniels, A. D.; Kudin, K. N.; Strain, M. C.; Farkas, O.; Tomasi, J.; Barone, V.; Cossi, M.; Cammi, R.; Mennucci, B.; Pomelli, C.; Adamo, C.; Clifford, S.; Ochterski, J.; Petersson, G. A.; Ayala, P. Y.; Cui, Q.; Morokuma, K.; Malick, D. K.; Rabuck, A. D.; Raghavachari, K.; Foresman, J. B.; Cioslowski, J.; Ortiz, J. V.; Baboul, A. G.; Stefanov, B. B.; Liu, G.; Liashenko, A.; Piskorz, P.; Komaromi, I.; Gomperts, R.; Martin, R. L.; Fox, D. J.; Keith, T.; Al-Laham, M. A.; Peng, C. Y.; Nanayakkara, A.; Gonzalez, C.; Challacombe, M.; Gill, P. M. W.; Johnson, B.; Chen, W.; Wong, M. W.; Anders, J. L.; Head-Gordon, M.; Replogle, E. S.; Pople, J. A.; Gaussian, Inc.: Pittsburgh, PA, 1998.

Table 2. Neutral Amines Used in Ion−Molecule Reactions

Neutral amine	Structure	Molecular weight	Proton affinity[56]
		g/mol	kJ/mol
methylamine	CH_3NH_2	31.04	899
dimethylamine	$(CH_3)_2NH$	45.06	929
ethylamine	$CH_3CH_2NH_2$	45.06	912
diethylamine	$(CH_3CH_2)_2NH$	73.09	952
triethylamine	$(CH_3CH_2)_3N$	101.12	982
n-propylamine	$CH_3CH_2CH_2NH_2$	59.07	917
cyclohexylamine		99.10	934

2000) on the Center for Scientific Computing (CSC) in Espoo. Optimization was carried out employing a restricted Hartree−Fock (RHF) procedure using the 3-21G basis set. Examination of binding geometries between the host and the guest (neutral amines) was done with Dock module within Sybyl.
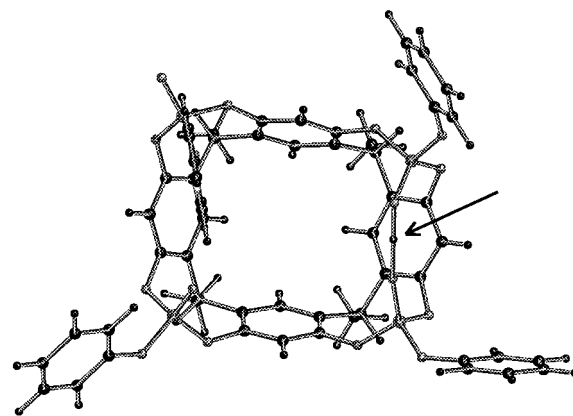
Sample Preparation. The synthesis and structural characterization of the cavitands studied are published elsewhere.[55] Acetonitrile, methanol, and water used in the experiments were all HPLC grade. Glacial acetic acid was used as a pH-modifier. The cavitands were first dissolved into acetonitrile at a concentration of 1 mg mL^{-1} (stock solution) and 10 μL of these solutions was diluted to 1 mL with a 70:30:1 methanol:water:acetic acid solution (sample solutions). The stock solutions were also diluted 100 times in methanol or acetonitrile with 1% acetic acid. All neutral amines (Table 2) were used without further purification; liquid amines were degassed by several freeze−pump−thaw cycles before introducing them into the vacuum system. Complex formation in solution for each cavitand was tested using 33% methylamine in ethanol and propylamine in 1:10, 1:1, and 2:1 cavitand:amine ratios, respectively. Alkali metal chlorides (LiCl, NaCl, KCl, RbCl, and CsCl) were dissolved in water and mixed with acetonitrile solutions of the cavitands in 10:1, 1:1, and 1:2 molar ratio. The alkali metal/cavitand mixtures were analyzed from methanol:water 7:3 or acetonitrile:water 8:2 solutions with and without acetic acid added.

Results and Discussion

Theoretical Results. The structure of the unprotonated cavitand **2b** carrying three inward and one outward oriented P=O groups was constructed and minimized using Sybyl. A systematic conformational analysis was carried out by rotating the two bonds of (P=O)−(O−p-tolyl) and (P−O)−p-tolyl of one phosphate group at a time in 2° increments. However, the starting structure resulted at the lowest energy conformation. In this conformation, the phenyl groups extended the walls of the cavity.

In ab initio calculations, cavitand **2b** was replaced by **1b**, to reduce the basis sets and, consequently, the calculation time. The geometry optimization using an RHF/3-21G basis set yielded a quite different structure from the one provided by molecular mechanics. The three phenyl substituents relative to inward-oriented P=O groups proved to point outside the molecular cavity while the distance between opposite inward P=O groups was 7.634 Å. This represent a reasonable value for a free molecule in comparison to the experimental value of 6.29 Å, found in the crystal structure of isomer **2d**. The orientation of phenyl substituents is determined by intramolecular hydrogen bonds between phenyl *ortho* hydrogens and oxygen atoms.

The optimized **1b** was protonated and the ab initio optimization was once again completed. In the final geometry, the proton was found to be situated in the middle (1.147 and 1.247 Å) of

(55) Lippmann, T.; Wilde, H.; Dalcanale, E.; Mavilla, L.; Mann, G.; Heyer, U.; Spera, S. *J. Org. Chem.* **1995**, *60*, 235−242.

Figure 1. Structure of the protonated **1b** after ab initio optimization. The arrow points the proton between two adjacent phosphate oxygens.

Table 3. Ions Observed in the ESI Mass Spectra Recorded from Methanol:Water:Acetic Acid (70:30:1) Solution of the Cavitands

	relative peak intensities of the ions in ESI spectra				
cavitand	[M + H]$^+$	[M + Na]$^+$	[M + K]$^+$	[M + H + H$_2$O]$^+$	[M + H + CH$_3$OH]$^+$
1b		28	17	50	100
2b		74	23	100	19
2c	7	94	29	31	100
2d	100	89	39	39	64
2e	100	56	7	6	12
2f	100	10	2	6	4
3b		100	53	32	4

two adjacent phosphate oxygens having almost linear hydrogen bonds (179.7°) (Figure 1). The overall cavitand structure is widely open, leaving the cavity easily accessible even for quite bulky guests. However, the cavitand is slightly compressed from square to rectangular. The distances between two carbon atoms of the opposite phenyl groups in the cavitand ring are quite different (6.996 and 9.284 Å) compared to the distances in unprotonated **1b** which were found to be around 8.2 Å in both cases.

The intrusion of neutral amines into the cavity was studied by molecular modeling using dock option, where neutral ethylamine and cyclohexylamine were selected to interact with the protonated cavitand **1b**. Both ethylamine and cyclohexylamine were found to dock both the amine and alkyl moiety inside the cavity without steric hindrance, forming an hydrogen bond between the amine nitrogen and the proton.

ESI Spectra of the Cavitands. Different solvents and solvent mixtures (methanol, acetonitrile, water) were tested for ESI measurements, with and without acetic acid. The best and most stable conditions were achieved when a 70:30 methanol:water solution with 1% acetic acid was used as the flowing solvent (Figure 2). The signal of the ESI spectra proved unstable without the presence of acetic acid, and also the peak intensities (especially the [M + H]$^+$ ion) were lower.

Table 3 reports the ion abundances observed in the ESI spectra of pure cavitands, recorded using a 70:30:1 methanol:water:acetic acid solvent. Most of the spectra, recorded using a low capillary voltage, exhibit the following ion peaks: [M + H]$^+$, [M + H + H$_2$O]$^+$, [M + H + CH$_3$OH]$^+$, [M + Na]$^+$, and [M + K]$^+$. No multiply charged ions were observed. It should be noted that the general features of the spectra remained the same from day to day, although the relative peak intensities varied slightly and the absolute intensities varied more considerably.
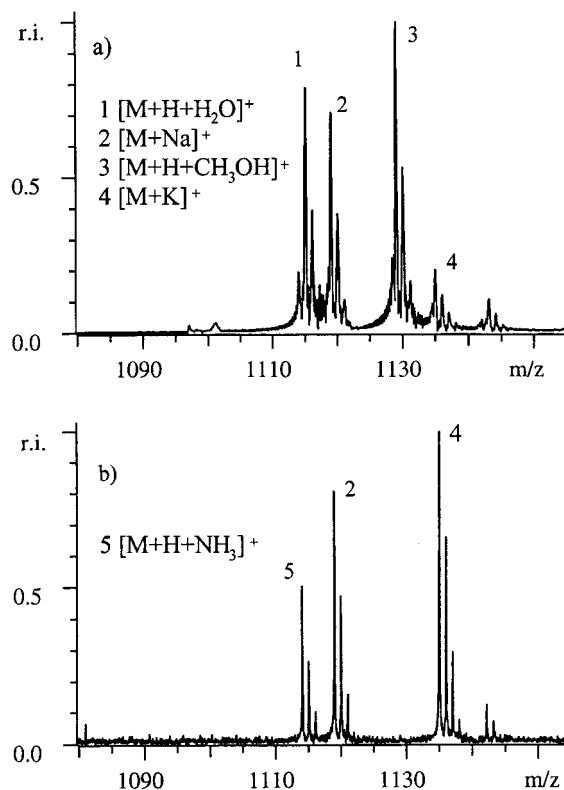
Figure 2. ESI spectra of cavitand **1b** recorded from (a) water:methanol 1:1 (v/v) solution with 1% acetic acid and (b) acetonitrile with 1% acetic acid.

Figure 3. ESI spectra of cavitand **1b** recorded from water:methanol: acetic acid 30:70:1 (v/v/v) solution using (a) 60 V and (b) 320 V capillary voltage.

Previous FAB investigations[46,48] proved that the five diastereo-isomers have a sharply decreasing ability to form inclusion complexes, from **2b** to **2f**. The ESI spectra show that the cavitands that form inclusion complexes in solution (**1b**, **2b**, **2c**, **3b**) give rise to intense $[M + H + H_2O]^+$ and $[M + H + CH_3OH]^+$ ion peaks. In contrast, the abundances of the $[M + H + H_2O]^+$ and $[M + H + CH_3OH]^+$ ions in the ESI spectrum of **2d** are significantly decreased and those in the spectra of **2e** and **2f** are extremely low. These results strongly confirm that real inclusion complexes with water and methanol are sampled in the gas phase for isomers **b**, **c**, and **d** but not for **e** and **f**. The formation of inclusion complexes depends on the structure of the cavitand isomer: the more P=O units directed toward the inside of the cavity, the more easily the inclusion complexes can be formed, and vice versa (Table 3). Complexes having water and methanol as guests were formed, especially with isomers **b** and **c**. The guest molecule is likely to be anchored to the host by multiple hydrogen bonds to the P=O moiety of the phosphate groups (P=O$_{host}$···H···O$_{guest}$).[29] The isomers **e** and **f**, not forming inclusion complexes, yield the $[M + H]^+$ ion as the most abundant ion in the ESI spectrum.

For all isomers, $[M + Na]^+$ and $[M + K]^+$ ions were formed from alkali metal ion impurities, but their intensities varied considerably from day to day. Despite daily variations, the average $[M + Na]^+$ and $[M + K]^+$ ion abundances showed some selectivity toward the isomers. Again, the abundances of alkali cationized molecular ions decreased as more P=O units were oriented outside the cavity. It is deduced that coordination of alkali metal ions outside the cavity is disfavored and, especially for isomer **b** and **c**, alkali cations should be located inside the cavity.

Different acetonitrile solutions were tested to prevent the formation of inclusion complexes between cavitands and the solvent. Even though $[M + H + CH_3CN]^+$ complexes were
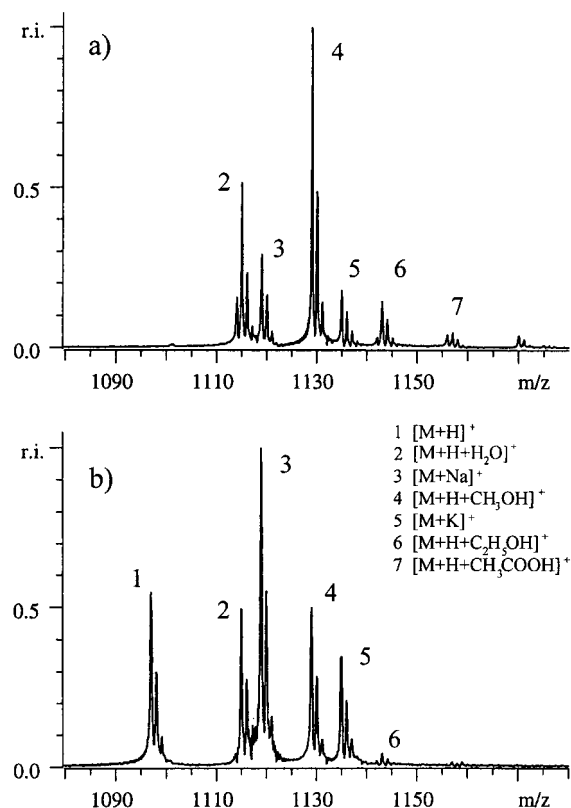
not observed in ESI spectra of acetonitrile:water:acetic acid 50:50:1 solutions, the intensity of $[M + H + H_2O]^+$, $[M + Na]^+$, and $[M + K]^+$ ion peaks became exceedingly large, while no $[M + H]^+$ ion was observed. The same occurred when pure acetonitrile with 1% acetic acid was used as the solvent (Figure 2b). These experiments also showed that ESI spectra of the cavitands are very sensitive to any impurity able to form hydrogen bonds, including ammonia, as is evident in Figure 2b.

To perform gas-phase reactions of protonated cavitands, it was necessary to form abundant $[M + H]^+$ ions from all isomers. Whenever scarce (as for isomer **b**), the formation of the $[M + H]^+$ ion was induced by decomposing $[M + H + H_2O]^+$ and $[M + H + CH_3OH]^+$ complexes. This was achieved by increasing the drying gas flow rate, by using a longer delay time in the hexapole or higher capillary voltages (in-source-CID) and by collision induced dissociation (CID) in the cell. Intensities of the $[M + H + H_2O]^+$ and $[M + H + CH_3OH]^+$ complexes gradually decreased as the capillary voltage was increased, to disappeare at the highest voltage (100 → 375 V) (Figure 3). In contrast, the complexes with sodium and potassium ions, $[M + Na]^+$ and $[M + K]^+$, did not decompose at high capillary voltages.

Complex Formation with Amines in Solution. The large differences encountered in ESI spectra for the various diastereo-isomers, particularly the variable abundance of $[M + H + H_2O]^+$ and $[M + H + CH_3OH]^+$ complex ions, indicate that inclusion complexes can be formed only for the cavitand isomers carrying two or more converging P=O units. To compare the FAB results previously obtained[46] with ESI data, cavitands and organic amines were dissolved together (as in FAB experiments) and the resulting acidic solutions were analyzed by ESI-MS. Methylamine and propylamine were utilized as candidate guests.
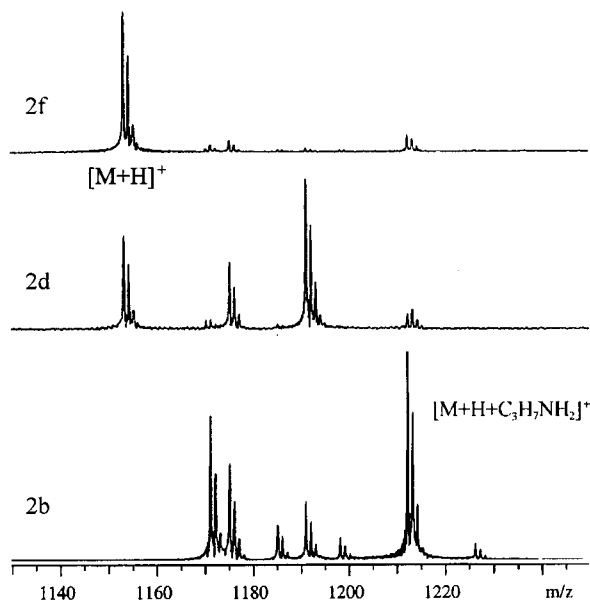
Figure 4. ESI mass spectra of equimolar cavitand−propylamine mixtures for cavitands **2b**, **2d**, and **2f** in water:methanol:acetic acid solvent.

Table 4. $[M + H + C_3H_7NH_2]^+/[M + H]^+$ Ratios Observed in the ESI Spectra Obtained by Mixing Equimolar Amount of Cavitands and Propylamine in Solution[a]

cavitand	$[M + H + C_3H_7NH_2]^+/$ $[M + H]^+$
2b	b
2c	1.37
2d	0.18
2e	0.11
2f	0.09

[a] Other ions were neglected. [b] Only the $[M + H + C_3H_7NH_2]^+$ ion was observed.

When each cavitand isomer (from **2b** to **2f**) was mixed with propylamine in 1:1 or 1:2 ratio, the resulting $[M + H + C_3H_7NH_2]^+$ ion became the base peak in the ESI spectrum for isomer **2b** only (Figure 4). Actually, the cavitand−propylamine complex ion was formed for most isomers but its abundance decreased continuously, as more P=O groups were oriented outside the cavity. The ratios between the inclusion complex ion and the empty cavitand ion for different isomers of cavitand **2** are presented in Table 4. The results clearly show that the affinity toward propylamine decreased in the order **2b** > **2c** > **2d** > **2e** > **2f**, although these results may not represent absolute affinity differences between the cavitands, since sodium and potassium ions were always present and competed with the amines for the binding site of the host. These results correlate well with both solution NMR data[55] and FAB measurements,[46] suggesting that both ESI and FAB reflect the equilibria of the corresponding liquid phases. Methylamine showed the same general behavior as $C_3H_7NH_2$ in ESI spectra of cavitand−amine mixtures. When the [amine]/[cavitand] molar ratio was increased, the specificity of complex formation was lost and the results approximated the trend observed in gas-phase reactions (see below). The $[M + H + C_3H_7NH_2]^+$ ion became the base peak in the spectrum of every diastereomer (**b**−**f**) when the [amine]/[cavitand] molar ratio was increased above 10:1. This effect is similar in all respects to that observed in FAB experiments.[46] Under these conditions, it was no longer possible to discriminate inclusion complexes from proton bound dimers. When a large excess of amine is introduced into the analytical
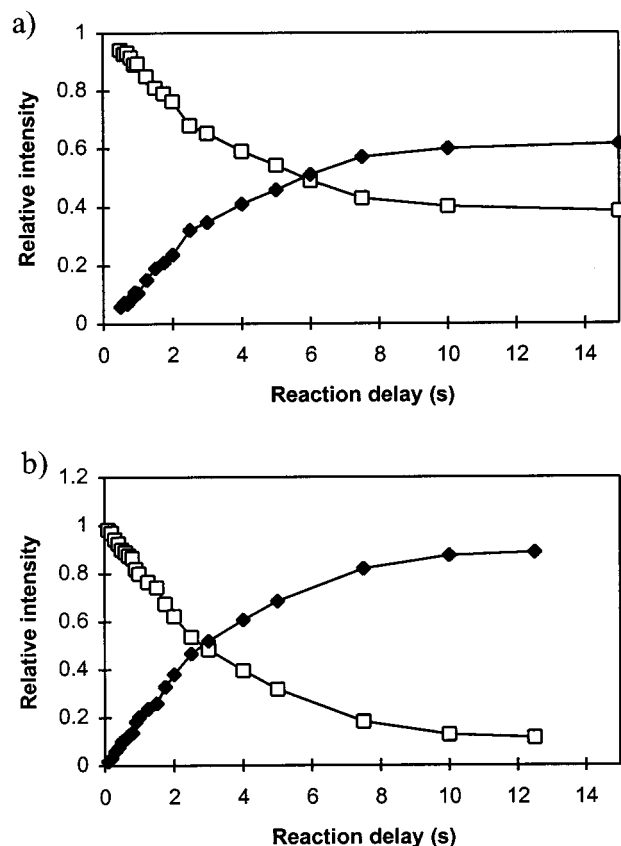

Figure 5. Relative peak intensities of the ions formed in the reaction between protonated (a) **2b** and (b) **2f** with neutral cyclohexylamine in the gas phase as a function of the reaction time. (◆ = [M + H + cyclohexylamine]$^+$ and □ = $[M + H]^+$.)

solution, the proton bound dimers are likely to be formed during the evaporation in the ESI process, as presented by Cunniff and Vouros.[45]

Gas-Phase Reactions of Cavitands with Neutral Amines. Reactions between cavitand diastereomers and organic amines were induced in the gas phase within the cell of the FTICR mass spectrometer. The cavitands were ionized, and the protonated $[M + H]^+$ ions were mass selected, isolated, and subsequently allowed to interact with gaseous neutral cyclohexylamine and propylamine for variable reaction periods until equilibrium was reached between reactant and product ions. Reactions were performed at different amine pressures to verify that real thermodynamic equilibrium was established in the cell. The effect of the P=O groups orientation in the cavitand on its gas-phase reactivity was investigated in detail. With every cavitand studied, the only ionic product ion observed was the $[M + H + amine]^+$ complex, i.e., protonated amine ions were not formed (Figure 5). The first part of the curves indicates that the reactions follow pseudo-first-order kinetics. The reaction efficiencies and the ratio between product and reactant ions in equilibrium were calculated (Table 5) and used to compare the behavior of different cavitand isomers.

Unlike solution data obtained by ESI and FAB,[46] the $[M + H + amine]^+$ product ion was formed for all **2** diastereomers reacting with neutral propylamine or cyclohexylamine in the gas phase, independently from the binding groups present inside the cavity. It is also noteworthy that the fastest reactions and the most favorable [product ion]/[reagent ion] ratios, $[M + H + amine]^+/[M + H]^+$, were observed for those isomers (**e** and **f**) that are not able to form inclusion complexes in solution. These results can be explained by assuming that either inclusion

Table 5. Reaction Efficiencies (k_{eff}) for the Reaction of [M + H]$^+$ Ions Generated from the Various Cavitands with Neutral Propylamine and Cyclohexylamine

amine		cavitand
		1b	2b	2c	2d	2e	2f	3b
cyclohexylamine	k_{teor}[a]	11.2	11.2	11.2	11.2	11.2	11.2	11.2
	k_{exp}[a]	2.5	3.7	2.5	8.8	9.3	11.1	6.7
	k_{eff}	**0.22**	**0.33**	**0.22**	**0.79**	**0.83**	**0.99**	**0.60**
	r[b]	2.2	2.3	c	9.8	7.1	7.8	7.8
propylamine	k_{teor}[a]	12.4	12.4	12.4	12.4	12.4	12.4	
	k_{exp}[a]	2.1	2.6	8.7	8.8	13.8	15.7	
	k_{eff}	**0.17**	**0.21**	**0.70**	**0.71**	**1.12**	**1.27**	
	r[b]	2.1	2.4	17.6	8.2	15.5	16.3	

[a] Rate constants in 10^{-10} cm^3/molecule s. [b] Ratio of the product ion and reactant ion when the reaction reaches equilibrium. [c] The measurement was stopped before equilibrium was reached as the signal became unstable.

Table 6. Reaction Efficiencies (k_{eff}) for the Reaction of the Cavitands **1b** and **2b** with Different Neutral Amines

amine	**1b** [M + H]$^+$		**2b** [M + H]$^+$	
	k_{eff}	[M + H + amine]$^+$/ [M + H]$^{+}$ [a]	k_{eff}	[M + H + amine]$^+$/ [M + H]$^{+}$ [a]
ethylamine	0.22	5.6	0.31	6.8
propylamine	0.17	2.1	0.21	2.4
cyclohexylamine	0.22	2.2	0.33	2.3
diethylamine	0.33	2.8	0.16	2.9
triethylamine	0.40	3.3	0.23	2.6

[a] Abundance ratio between the product ion and the reactant ion when the reaction reaches equilibrium.

complexes or proton bound dimers are alternatively formed in these experiments, the choice depending on the isomer structure. The lowest reaction efficiency was observed for the isomer **2b** and increased as more P=O units were oriented toward the outside of the cavity, following the order **b** < **c** = **d** < **e** < **f**. For isomers **f** and **e**, ion−molecule reaction took place at the collision rate. The most basic position for proton attachment in all cavitands is the oxygen of the P=O unit, as demonstrated by CID experiments (see below).[29,46] When all these groups are oriented outside the cavitand (isomer **f**), the proton must also be situated outside the cavity and fast formation of a proton bound dimer is likely to occur. With isomer **b**, where three of the four P=O groups are oriented inside the cavity, the proton must also be situated inside the cavity, due to the synergistic effect of multiple hydrogen bonding. Thus, the neutral amine is forced to go inside the cavity in order to coordinate the same proton. Quite obviously, this reaction, namely, inclusion complexation, involves multiple coordination, which may slow the reaction rate as compared to proton-bound dimerization occurring outside the cavity.

Figure 5a also shows that the reaction of neutral propylamine with isomer **2b** is incomplete, whereas that with isomer **2f** reaches completeness. This thermodynamic effect can be rationalized by considering that, while multiple hydrogen bonds are formed between the P=O groups of isomer **b** and the proton, only one hydrogen bond is formed between the proton and the amine. Moreover, this hydrogen bond is rather weak, as the multiple P=O···H interactions partly compensate the H$^+$ charge polarization. The resulting effect is a strong proton affinity of the cavitand, so that the proton bridging the cavitand and the amine in the host−guest complex gets strongly polarized toward the cavitand oxygens with little electron vacancy remaining for the amine nitrogen. Some conformational strain associated with inclusion complexation could further contribute to make the interaction between the *protonated* isomer **2b** and a *neutral* amine rather weak and thermodynamically unstable. In contrast, an interaction between the *neutral* isomer **2b** and a *protonated* amine should be thermodynamically favorable, since several hydrogen bonds are formed simultaneously in the process. This phenomenon has, in fact, been ascertained by solution FAB and ESI experiments. Another consequence of the present explanation is that cavitands **1b**, **2b**, **2c**, and **3b** must be stronger bases than propylamine. This deduction is confirmed by the CID experiments discussed in the forthcoming section.

The results presented in Table 5 also show that the reaction efficiencies of **2b** with both neutral propylamine and cyclohexylamine are practically the same. This suggests that the size of the amine is irrelevant to the inclusion complexation, which, in turn, indicates that the cavity of the host is quite large and accessible in the gas phase as already observed by ab initio calculations. In contrast, the formation of proton bound dimers with cyclohexylamine (isomer **2f**) proved to be slightly slower than that with propylamine. This difference can be explained by the higher proton affinity of cyclohexylamine, which makes the proton-bound dimer formation more exothermic than with propylamine. The excess of internal energy accumulated on the complex might induce partial decomposition reforming the reactants. The same phenomenon is also reflected in a smaller [M + H + amine]$^+$/[M + H]$^+$ ratio for cyclohexylamine than for propylamine.

By comparing [M + H + amine]$^+$/[M + H]$^+$ ratios and efficiencies for the reaction between neutral cyclohexylamine and cavitands **1b**, **2b**, and **3b** (Table 5), all leading to the formation of inclusion complexes, it is deduced that the introduction of a methyl group (R = CH$_3$) on the aryl substituents of the cavitand phosphates has little effect on its reactivity. In fact, cavitands **1b** and **2b** exhibit very similar k_{eff} and r values, which also supports that the cavitand has an open and accessible reacting conformation. On the other hand, cavitand **3b**, carrying four bulky *tert*-butyl groups on the upper rim of the cavity, reacts significantly faster than **1b** and **2b** with cyclohexylamine and, most important, the reaction equilibrium is considerably shifted toward complexation. Since purely kinetic factors cannot justify this difference (bulky substituents should increase the steric hindrance and decrease, not increase, the kinetics), the faster and more extensive reaction for **3b** is perhaps a consequence of a more effective electron-donating character of the C(CH$_3$)$_3$ groups as compared to the CH$_3$ groups in **2b**.

Further study on the effect of the amine structure on inclusion complex formation was conducted by reacting cavitands **1b** and **2b** with mono-, di-, and triethylamine. The reaction efficiencies was found to be approximately the same for all these amines and also for propylamine and cyclohexylamine (Table 6), confirming that the kinetics for inclusion complex formation is similar for all these guests and thus independent of steric factors. On the other hand, the [product ion]/[reactant ion] ratio (see Experimental Section), [M + H + amine]$^+$/[M + H]$^+$, is approximately the same for all the amines studied with the exception of ethylamine which yields a higher value. In principle, for reactions under identical conditions the [M + H + amine]$^+$/[M + H]$^+$ ratio at equilibrium position should reflect the relative stability of the complexes formed. If the amines were allowed to form multiple hydrogen bonds with the converging P=O groups of cavitands **1b** and **2b**, then the stability order for inclusion complexes should have been primary amine > secondary amine > tertiary amine, because of the aminic hydrogens still available to form additional bonds with the remaining two P=O groups inside the cavity. This dependence of the complex stability on the amine structure has not

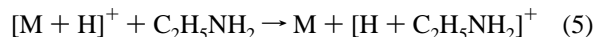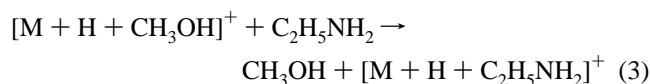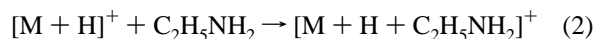**Table 7.** Reaction Efficiencies, k_{eff}, of the $[M + H + CH_3OH]^+$ Ions with Neutral Amines

cavitand	neutral	product ions[a]	k_{eff}
1b	$CH_3CH_2NH_2$	$[CH_3CH_2NH_2 + H]^+$, 4; $[M + H]^+$, 4; $[M + H + CH_3CH_2NH_2]^+$, 92	0.33
2b	$CH_3CH_2NH_2$	$[CH_3CH_2NH_2 + H]^+$, 9; $[M + H]^+$, 8; $[M + H + CH_3CH_2NH_2]^+$, 83	0.39
1b	$(CH_3CH_2)_2NH$	$[(CH_3CH_2)_2NH + H]^+$, 10; $[M + H]^+$, 4; $[M + H + (CH_3CH_2)_2NH]^+$, 86	0.27
2b	$(CH_3CH_2)_2NH$	$[(CH_3CH_2)_2NH + H]^+$, 11; $[M + H]^+$, 0; $[M + H + (CH_3CH_2)_2NH]^+$, 89	0.44
1b	$(CH_3CH_2)_3N$	$[(CH_3CH_2)_3N + H]^+$, 15; $[M + H]^+$, 4; $[M + H + (CH_3CH_2)_3N]^+$, 81	0.53
2b	$(CH_3CH_2)_3N$	$[(CH_3CH_2)_3N + H]^+$, 10; $[M + H]^+$, 8; $[M + H + (CH_3CH_2)_3N]^+$, 82	0.64
1b	$C_6H_{11}NH_2$	$[C_6H_{11}NH_2 + H]^+$, 55; $[M + H]^+$, 0; $[M + H + C_6H_{11}NH_2]^+$, 45	0.58
2b	$C_6H_{11}NH_2$	$[C_6H_{11}NH_2 + H]^+$, 10; $[M + H]^+$, 8; $[M + H + C_6H_{11}NH_2]^+$, 82	0.60

[a] Intensities at equilibrium.
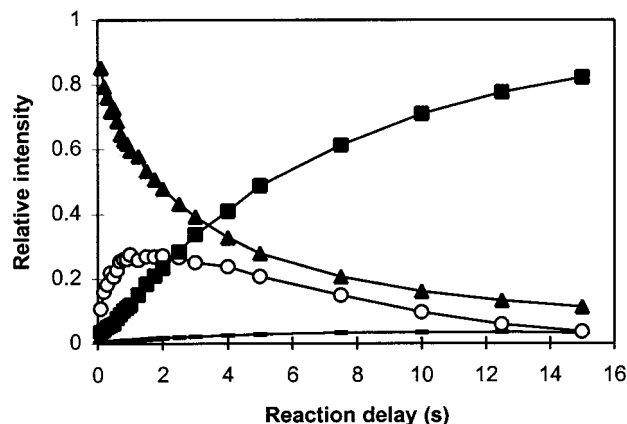
Figure 6. Relative peak intensities of the ions formed in the reaction of $[M + H + CH_3OH]^+$ ion generated from **1b** in methanol solution with ethylamine as a function of the reaction time. (▲ = $[M + H + CH_3OH]^+$, ■ = $[M + H + CH_3CH_2NH_2]^+$, ○ = $[M + H]^+$ and − = $[CH_3CH_2NH_2 + H]^+$.)

been observed, as the anomalous value obtained for the primary ethylamine is not confirmed by the consistent value observed for propylamine. The fact that the $[M + H + amine]^+/[M + H]^+$ ratios are the same for primary, secondary, and tertiary amines strongly supports the hypothesis that only one hydrogen bond is formed between the nitrogen lone electron pair and the proton bound to multiple P=O groups. Thus, two or perhaps three P=O groups are involved in the coordination of the proton and are unavailable to form additional hydrogen bonds with the aminic hydrogens. Partial hydrogen bonding could possibly be established between the third P=O group and aminic hydrogens, but this effect is likely to be balanced by the higher proton affinity of tertiary amines. It is still possible that several weak CH···π interactions between the aliphatic part of amines and the aromatic walls of the cavitand stabilize the complexes. A more efficient distribution of such additional interactions may explain the complex stability differences between ethylamine and propylamine complexes.

Some guest-substitution reactions were also studied for **1b** and **2b** using four different neutral amines to replace methanol from $[M + H + CH_3OH]^+$ ions (Table 7). Care had to be taken during the isolation of the $[M + H + CH_3OH]^+$ ions because they dissociated easily to form $[M + H]^+$ ions. This proves that methanol is weakly bound to the cavitand as already observed by in-source-CID experiments. However, without collisional activation $[M + H + CH_3OH]^+$ proved stable, as it could be trapped for 20 s periods without producing any detectable $[M + H]^+$ ion. It is reasonable to assume that the $[M + H + CH_3OH]^+$ ions represent real inclusion complexes because their existence correlates with the inclusion complex formation observed in solution, as discussed above. Figure 6 shows the intensities of the ions formed in the reaction of

ethylamine with $[M + H + CH_3OH]^+$ (generated from **1b**) as a function of the reaction time. The amine complexes, namely $[M + H + amine]^+$ ions, are supposed to be formed through the sequence of reactions presented in eqs 1−3 below. At short reaction times, $[M + H]^+$ ions are formed as the most abundant product by elimination of a methanol molecule (reaction 1). The formation of $[M + H + amine]^+$ ions results from both the reaction of $[M + H]^+$ ions with neutral amine (reaction 2) and to ligand switching reaction (reaction 3). Both mechanisms are consistent with the observed increment of the abundance ratio $[M + H + CH_3OH]^+/[M + H + C_2H_5NH_2]^+$, when the pressure of ethylamine was decreased. Protonated amine ions were also produced although their abundance was generally low. These ions could be formed through reactions 4 and 5.

$$[M + H + CH_3OH]^+ \rightarrow CH_3OH + [M + H]^+ \quad (1)$$

$$[M + H]^+ + C_2H_5NH_2 \rightarrow [M + H + C_2H_5NH_2]^+ \quad (2)$$

$$[M + H + CH_3OH]^+ + C_2H_5NH_2 \rightarrow$$
$$CH_3OH + [M + H + C_2H_5NH_2]^+ \quad (3)$$

$$[M + H + C_2H_5NH_2]^+ \rightarrow M + [H + C_2H_5NH_2]^+ \quad (4)$$

$$[M + H]^+ + C_2H_5NH_2 \rightarrow M + [H + C_2H_5NH_2]^+ \quad (5)$$

The results observed for $[M + H + CH_3OH]^+$ ions partially differ from the ones observed for $[M + H]^+$ ions, which is not surprising since the reaction mechanisms are different. The reaction efficiencies are slightly higher than with $[M + H]^+$ ions, although in both cases they were very close for all of the amines studied. The largest difference, however, is observed for [product ion]/[reactant ion] ratio, as almost all $[M + H + CH_3OH]^+$ ions did react to give product ions. This result is coherent with the hypothesis that the inclusion complex formed by methanol is significantly weaker than those formed by amines. The guest substitution reaction is likely to involve a favorable enthalpic contribution as well as a positive entropy change associated with the methanol release because due to the large excess of neutral ethylamine its concentration does not change significantly. Another reason for the complete reaction of the methanol complex relates to the energy transfer for the reaction: the multiple coordination undergone by the $[M + H]^+$ ions produces an excess of energy, which is possibly released on the $[M + H + C_2H_5NH_2]^+$ product by activating the back reaction. In contrast, the $[M + H + CH_3OH]^+$ complex can lose the excess of energy with the release of the CH_3OH molecule.

Collision-Induced Dissociation. Collision-induced dissociation experiments were carried out by increasing collision energy, to obtain breakdown plots and to determine the relative stability of the inclusion complexes formed from various cavitands under
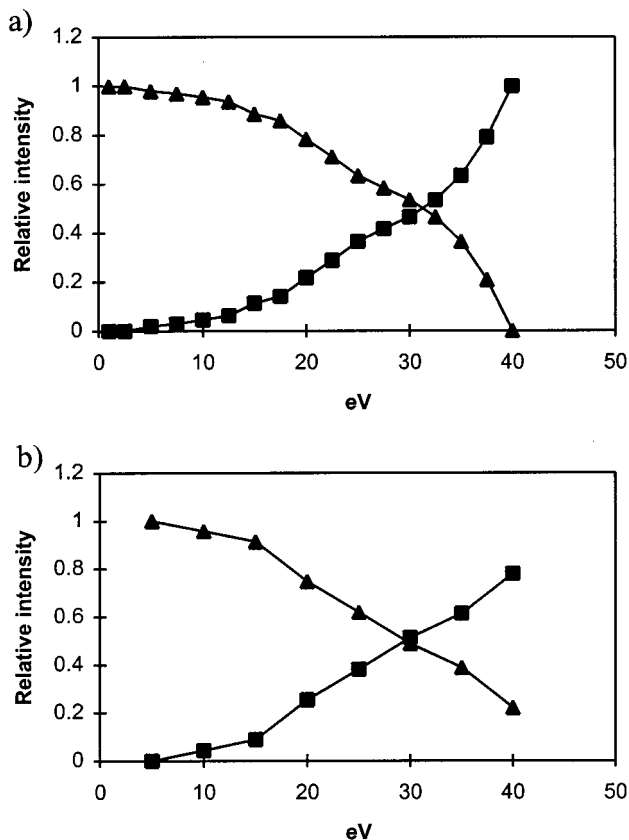
a)

b)

Figure 7. Breakdown graphs reporting the relative abundance of the ions formed by collision induced dissociation of the [**2b** + H + propylamine]$^+$ ion, as a function of the collision energy. The charged host−guest complex is formed (a) by ESI of a solution obtained by mixing **2b** and propylamine in 1:1 molar ratio and (b) in the gas phase by the reaction between the [M + H]$^+$ ion and neutral propylamine. (▲ = [M + H + propylamine]$^+$ and ■ = [M + H]$^+$.)

a)

b)

Figure 8. Breakdown graphs reporting the relative abundance of the ions formed by collision induced dissociation of the [**2f** + H + propylamine]$^+$ ion, as a function of the collision energy. The adduct is produced (a) by ESI of a solution obtained by mixing **2f** and propylamine in a 1:10 molar ratio and (b) in the gas phase by the reaction between the [M + H]$^+$ ion and neutral propylamine. (▲ = [M + H + propylamine]$^+$, ○ = [propylamine + H]$^+$, and ■ = [M + H]$^+$.)

different conditions. Two different isomers, **2b** and **2f**, were selected for comparative experiments, since they were expected to form pure inclusion complexes and proton bound dimers, respectively. CID spectra were obtained from the complexes of **2b** and **2f** with propylamine, formed by both gas-phase reactions and electrospray ionization. For cavitand **2b**, the breakdown graphs were very similar for the complexes prepared by ESI and by gas-phase reaction, indicating that the structure of the complex is identical in the two cases. The [M + H + C$_3$H$_7$NH$_2$]$^+$ complex ions dissociated by eliminating the neutral propylamine yielding [M + H]$^+$ ions as the unique charged product (Figure 7). This result confirms once more the high proton affinity of **2b**. In a previous study,[46] the gas-phase proton affinity of triphenylphospate could be measured precisely (900.6 kJ mol^{-1}) by the kinetic method,[57,58] as it proved intermediate between those of *p*-anisidine (900.3 kJ mol^{-1})[59] and 2-chloro-pyridine (900.9 kJ mol^{-1}),[59] while the proton affinity of **1b** could only be roughly estimated (about 945−950 kJ mol^{-1}) as largely exceeding that of cyclohexylamine (934.4 kJ mol^{-1}),[59] given the restrictions of the method itself. It has to be noted that the kinetic method assumes that the transition states are similar for the two competing dissociations, which is not completely true

for the present case. In fact, the proton is coordinated by two P=O groups in the host, but has a single bond with the amine hydrogen of the guest.

The interaction product of isomer **2f** with propylamine showed a radically different decomposition path (Figure 8). In CID product ion spectra, the most important product ion is the protonated propylamine. This result clearly indicates that the gas-phase proton affinity of **2f** is lower than that of propylamine, as expected. At higher collision energies, the [M + H]$^+$ ions also appeared in the CID product spectrum, but only from the [M + H + C$_3$H$_7$NH$_2$]$^+$ complex generated by ESI from a solution of mixed reagents, whereas the [M + H]$^+$ fragment ions were not present in CID spectrum of the complex prepared in the gas phase. This difference is most likely not due to distinct structures of the complexes generated by different processes, but rather reflects the occurrence of a gas-phase back reaction of the [M + H]$^+$ ion with propylamine to produce the [M + H + C$_3$H$_7$NH$_2$]$^+$ precursor ion. It is also important to note that the isomer **2b** needed more than two times higher collision energy than **2f** to dissociate to equally abundant precursor and product ions, (about 30 eV for **2b** and about 12 eV for **2f**). This energy difference reflects the higher stability of the inclusion complex generated from cavitand **2b** with respect to the proton-bound dimer generated from **2f**. The easy dissociation route existing for the **2f**−propylamine adduct to give the protonated propylamine, which cannot be observed in ion−molecule reactions, explains why such an adduct appears to be less stable than the **2b**−propylamine inclusion complex (from

(56) NIST Chemistry WebBook, http://webbook.nist.gov/chemistry/ 24.11.1998.

(57) Cooks, R. G.; Kruger, T. L. *J. Am. Chem. Soc.* **1977**, *99*, 1279−1281.

(58) McLuckey, S. A.; Cameron, D.; Cooks, R. G. *J. Am. Chem. Soc.* **1981**, *103*, 1313−1317.

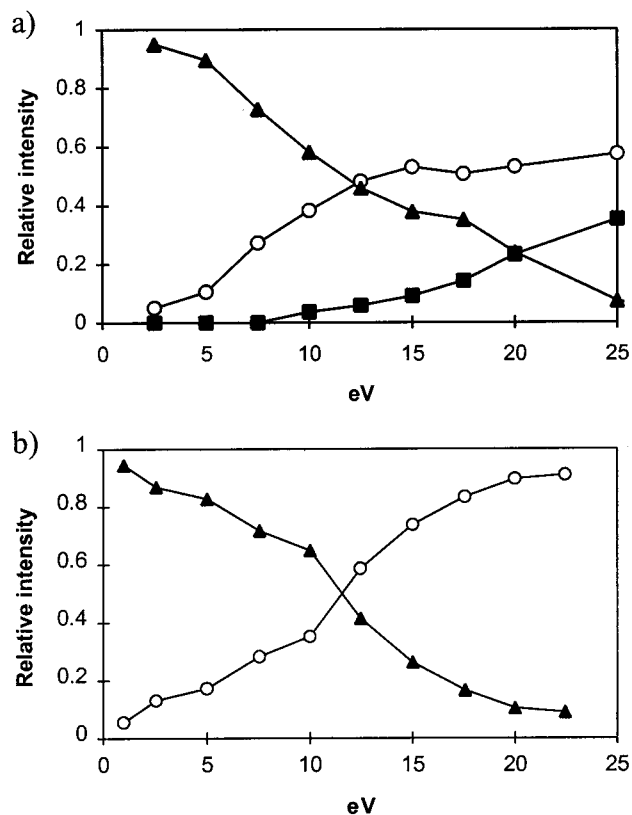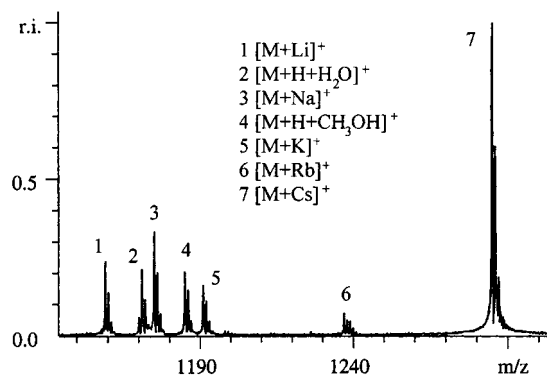(59) Hunter, E. P.; Lias, S. G. *J. Phys Chem. Ref. Data* **1998**, *27*, 413.

Figure 9. ESI mass spectrum representing the product ion distribution formed by dissolving equimolar amounts of each alkali metal chloride (LiCl, NaCl, KCl, RbCl, and CsCl) with cavitand **2b** in a methanol: water 7:3 (v/v) solvent.

CID experiments), while the opposite was deduced from gas-phase ion−molecule reaction experiments.

Complexation of Alkali Metal Ions in Solution. It was previously observed that $[M + Na]^+$ and $[M + K]^+$ ion peaks appeared in the ESI spectra of the cavitands obtained without the addition of the corresponding salts. This finding suggested to us to test the ability of cavitands **2b** and **2f** to selectively form complexes with different alkali metal cations (Li^+, Na^+, K^+, Rb^+, Cs^+) in solution. The most favorable binding site for **2b** is inside the cavity, whereas for **2f** the interaction must take place outside the cavity. The relative affinity of alkali metal cations for cavitand **2b** was also studied by dissolving it with equimolar amounts of an alkali metal chloride mixture.

As already observed in the data of Table 3, adduct ion formation between alkali metal cations and cavitand **2f** is unfavorable. Only rubidium and cesium ions formed observable adducts with **2f**; however, their signal remained weak.

Cavitand **2b** exhibited a quite large degree of selectivity in the complexation of alkali cations. By dissolving **2b** and cesium chloride at a 1:1 concentration ratio in water−methanol−acetic acid solution, the base peak in the ESI spectrum was the $[M + Cs]^+$ complex ions while the other signals, corresponding to $[M + H + H_2O]^+$ and $[M + H + CH_3OH]^+$ complex ions, had an intensity lower than 15% of the base peak. By using rubidium instead of cesium, the $[M + Rb]^+$ complex still represented the base peak in the ESI spectrum; however, water and methanol complexes also produced intense signals. Considerably less abundant alkali metal complexes were formed with lithium, sodium, and potassium and did not even represent the base peaks in the corresponding ESI spectra. Differences in ionization efficiencies and mass discrimination effects are expected to be limited for inclusion complexes formed between a large host and a relatively small guest already carrying a charge.[60]

The experiments of competitive complexation, where cavitand **2b** was dissolved with a mixture of alkali metal ions, provided a slightly different picture (Figure 9) than when only one metal cation was used. The degree of complexation for the alkali metal ions followed the order Cs ≫ Na > Li > K > Rb. However, when acetonitrile was used as a cosolvent in place of methanol, the expected order of complexation efficiency was reestablished: Cs ≫ Rb > K ≥ Na ≥ Li. The strong affinity of cesium ion toward **2b** is explained by its large ionic radius being complementary to the cavity size. This allows cesium to be bound by all three adjacent P═O groups present inside the cavity

of **2b**. The high affinity for cationic species by a iiii tetraphosphonate cavitand in organic solution has been reported.[61] Smaller alkali metal cations are likely to be efficiently coordinated by only two adjacent P═O groups, with the third binding site playing a decreasing role along the series.

Conclusions

The solution- and gas-phase reactivity of a new class of phosphate-bridged cavitands toward a series of alkylamines has been studied. The cavitands were organized in series of diastereoisomers differing from one another only for the spatial orientation of the monomeric units forming their tridimensional structure. As the main reacting sites for each cavitand are the unsaturated oxygens of the four phosphate groups present in its structure, the outstanding reactivity differences encountered experimentally among isomers could be attributed to the relative orientation of these P═O groups. The presence of multiple P═O oxygens converging toward the center of the cavity (isomers **b**, **c**, and **d**) gives rise to cooperative binding, high proton affinity, and formation of inclusion complexes.

Several experimental findings confirm the synergistic effect of multiple binding, leading to strong inclusion complexation, while only weak proton-bound adducts are occasionally formed between alkylamines and the cavitands carrying three or four P═O groups oriented toward the outside of the structure (isomers **e** and **f**). These results include (i) previous NMR and FAB-MS data indicating the formation of 1:1 complexes in solution only for isomers **b** and, to a minor extent, **c** and **d**; (ii) ESI mass spectra of the cavitand isomers, showing extensive association of one solvent molecule by isomer **b** and strong dependence of the abundance of such complex on the number of in-pointing phosphates; (iii) ESI mass spectra of 1:1 cavitand−amine solutions, again showing strong correlation of the peaks corresponding to 1:1 adducts with the number of in-pointing P═O groups in the cavitand structure; (iv) CID mass spectra, indicating that the proton affinity of propylamine is much lower than that of isomer **b** and higher than that of isomer **f**; (v) energy-resolved collisional activation experiments, demonstrating that the collision energy required to dissociate one-half of the [isomer **b**···H···propylamine]$^+$ complexes is 30 eV, whereas that needed to dissociate the [isomer **f**···H···propylamine]$^+$ adduct is only 12 eV; (vi) kinetic measurements, showing much faster gas-phase reactions between protonated cavitands and alkylamines for isomers **e** and **f**, which are presumed to carry the proton externally; (vii) ESI mass spectra of equimolar cavitand−alkali metal ion solutions, exhibiting extensive formation of 1:1 complexes for isomer **b**, not for isomer **f**; (viii) molecular model calculations, showing that the isomer **b** has a wide and open cavity, readily accessible even for bulky guests.

Further experimental results, which appear controversial from immediate evaluation, can be explained coherently with the preceding interpretation scheme. These include (i) FTICR equilibrium measurements for charged cavitands reacting with neutral alkylamines, showing more favorable formation of 1:1 adducts for isomers **e** and **f** than for isomers **b**, **c**, and **d**; (ii) the absence of steric hindrance effects on complexation kinetics and equilibria due to the reaction with bulky guests and the addition of bulky substituents on the upper rim of the cavity; (iii) the similarity of kinetic and equilibrium results for primary, secondary, and tertiary amines reacting with the charged isomer **b**. The latter results are explained by considering that the

(60) Ralf, S. T.; Iannitti, P.; Kanitz, R.; Sheil, M. M. *Eur. Mass Spectrom.* **1996**, *2*, 173−179.

(61) Delangle, P.; Dutasta, J.-P., *Tetrahedron Lett.* **1995**, *36*, 9235−9328.

10100   *J. Am. Chem. Soc., Vol. 122, No. 41, 2000*

Nuutinen et al.

synergistic effect of three converging binding groups in isomer **b** produce a strong coordination of the proton but have little effect on the subsequent interaction with the neutral amine, being coordinated by a single polarized hydrogen bond. The absence of steric hindrance is confirmed by molecular calculations showing that isomer **b** has a wide and open cavity.

The whole set of results obtained for the class of cavitands studied represent a striking example of the importance of cooperative interactions in determining the chemical properties of molecular receptors. The synergistic behavior of an increasing number of convergent P=O groups drastically enhances com-plexation properties and proton affinities of the corresponding cavitands with respect to the other diastereomers.

JA000486J